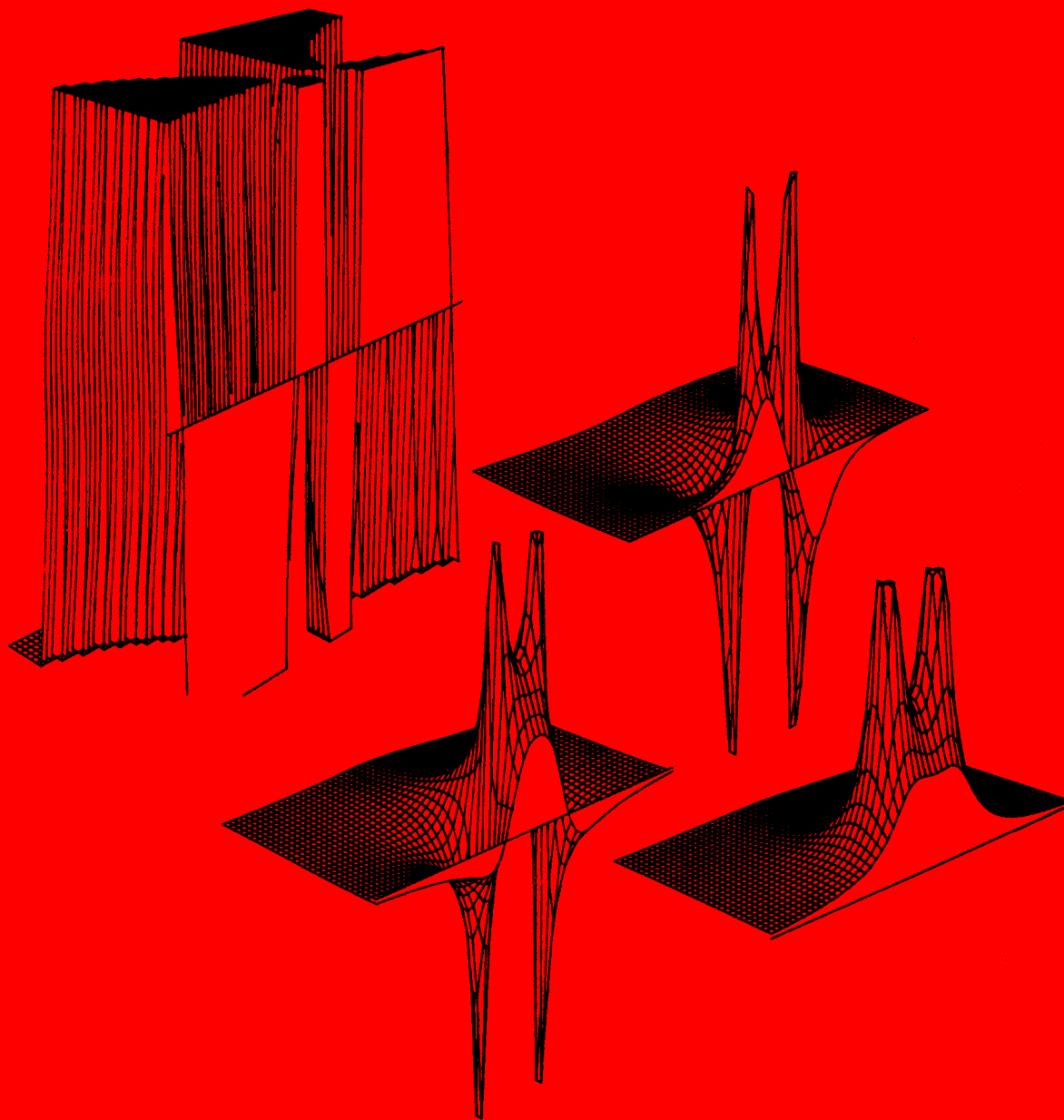


# APPLICATION NOTE

## DIGITAL SIGNAL ANALYSIS

Feedback Control System Measurements



240-1



The Hewlett-Packard 5420A Digital Signal Analyzer utilizes sampled data techniques to perform a wide variety of single and dual channel measurements over a 25 kHz frequency range. Measurements include Time Record Averaging, Auto and Cross Correlation, Impulse Response, Auto and Cross Spectrum, Transfer Function and more. Important features include Band Selectable Analysis, which provides excellent frequency resolution, and built-in data storage on digital magnetic tape cartridges. The instrument also contains a random noise generator, which is useful as a test stimulus, and it provides a fully-annotated dual-trace display with flexible cursor capabilities.

The 5420A is directly compatible with the HP Models 9872C, 7245B, and 7225A/17601A Graphics Plotters. Any of these plotters may be used to obtain alphanumeric and annotated graphic hardcopy for reports and record keeping. The 5420A also features an HP-IB Interface to allow for control by and data transfer to external calculators or computers.

#### ON THE COVER

*The cover illustrations are complex s-plane plots of the control system model discussed on page 3. They were generated by programming an HP Model 9825A Desktop Computer to evaluate Equation 9 over a portion of the left half of the s-plane and to plot the results on a Model 9872A Graphics Plotter.*

## Introduction

The advantages which closed-loop feedback control systems offer relative to simpler open-loop control schemes have long been recognized. Benefits to be gained include faster and more accurate response to control signals, reduced sensitivity to component variations, and improved compensation for load variations. As a result, closed-loop control is used in applications ranging from the simple 'bang-bang' thermostat found in the home to sophisticated, multivariate, industrial process control.

The ability to quickly, conveniently, and completely characterize such systems is extremely important as it can aid in verifying and optimizing the design, maximize production, and ease maintenance and troubleshooting. The Hewlett-Packard Model 5420A Digital Signal Analyzer can make substantial contributions to the measurement of feedback control systems.

## The Classical Feedback Model

Before examining these contributions in detail, let's begin by reviewing the classical, single-loop, feedback control system illustrated in Figure 1. The diagram shows the system to consist of a forward transmission path labeled  $G(j\omega)$ , a feedback path labeled  $H(j\omega)$ , and a summing node. The second summing node, with input  $S(j\omega)$ , represents system noise and load variation modeled as an undesired input to an otherwise ideal system. The system can be described in either the time or frequency domain. If the system is linear the time and frequency domain descriptions are equivalent in a mathematical sense, although various characteristics may be more easily studied in one domain than the other. As will be illustrated, the 5420A is well suited to making either class of measurements and the user is free to choose the technique which yields the most meaningful result.

Assuming linearity, each block in the system can be uniquely described by its transfer function. In addition, there is an overall transfer function which results from considering the dotted line in Figure 1 to enclose a black box with  $R(j\omega)$  as the input and  $C(j\omega)$  the output. If we ignore  $S(j\omega)$  for the moment, the closed-loop transfer function for this system can be expressed in terms of the component functions as:

$$\frac{C(j\omega)}{R(j\omega)} = \frac{G(j\omega)}{1 + G(j\omega)H(j\omega)} \quad (1)$$

The product  $G(j\omega)H(j\omega)$  is important enough to be given a name, the open-loop transfer function. It determines the most important parameters of the closed-loop system including absolute and relative stability. Absolute stability is important as without it the system is useless while relative stability is a measure of the margin available before absolute stability is lost. In addition, there is a close relationship between relative stability and the transient response of a system.

We will use the Nyquist criteria which states that, for the system to be closed loop stable, the real/imaginary plot of  $G(j\omega)H(j\omega)$  must not enclose the point  $-1 + j0$  in the complex plane as our measure of absolute stability. Relative stability will be gauged by the gain and phase margins. The gain margin is the reciprocal of  $G(j\omega)H(j\omega)$  at the frequency where its phase is 180 degrees. The phase margin is  $180^\circ - \angle G(j\omega)H(j\omega)$  at the frequency where the magnitude of  $G(j\omega)H(j\omega)$  is unity (0 dB).

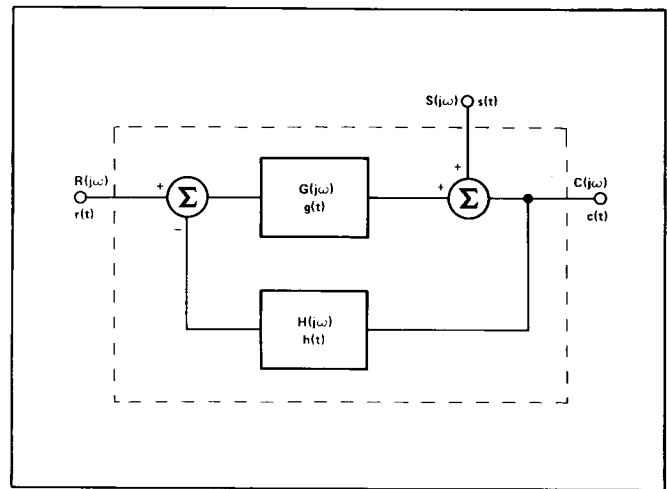


Figure 1

## The Traditional Measurement Approach

The measurement of  $G(j\omega)H(j\omega)$  is frequently carried out with the loop open and the control system inoperative. Sinusoidal excitation is applied to the input and the magnitude and phase at the output is recorded for frequencies of interest. This technique, while usually valid, suffers from several practical disadvantages.

- The gain being measured is, typically, quite high particularly at low frequencies. This places severe dynamic range requirements on the test equipment and makes the task of maintaining an adequate signal-to-noise ratio difficult.
- The system will often be non-linear. Analysis frequently assumes linearity around some nominal operating point, but a sinusoidal input is a poor stimulus to choose for approximating this condition, particularly with the loop open and the system inoperative.
- Long system time constants require long settling times each time the frequency is changed. The designer must devote substantial time to gathering the data he needs.

- Some systems cannot be operated open loop, particularly with a sinusoidal input.
- Most conventional test equipment which is suited to making such measurements is poorly equipped to display, plot, store, and process the results in a convenient and useful fashion. Additional manual labor and time are required to interpret the data.

## A Closed-Loop Approach Using Random Noise

The Hewlett-Packard Model 5420A Digital Signal Analyzer can substantially overcome all of these drawbacks of conventional techniques. Examination of the disadvantages listed reveals that the first four could be eliminated if a method can be found whereby the measurement is made with the loop closed and if a more satisfactory stimulus can be utilized. The final objection can be overcome by using instrumentation which takes advantage of today's powerful and low-cost digital technology with its considerable ability to manipulate data.

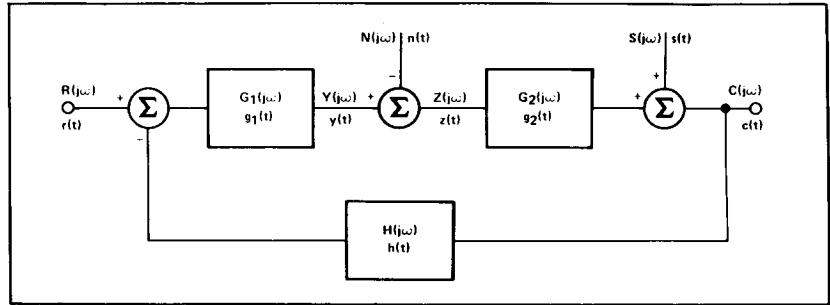


Figure 2

Figure 2 illustrates a modification to the system illustrated in Figure 1. The forward transmission path  $G(j\omega)$  has been represented as two blocks,  $G_1(j\omega)$  and  $G_2(j\omega)$ , separated by a newly introduced summing node. There is no loss of generality here since:

$$G(j\omega) = G_1(j\omega)G_2(j\omega) \quad (2)$$

and, in fact, this represents a common situation where  $G_1(j\omega)$  is a high gain error amplifier and  $G_2(j\omega)$  is an actuator.  $N(j\omega)$  is a test signal input to the new summing node. This node could be placed anywhere inside the loop, but is typically placed for optimum signal-to-noise ratio. We can write:

$$Y(j\omega) = - \frac{[Y(j\omega) - N(j\omega)]G_1(j\omega)G_2(j\omega)H(j\omega)}{-S(j\omega)G_1(j\omega)H(j\omega) + R(j\omega)G_1(j\omega)} \quad (3)$$

and, solving for  $Y(j\omega)$ :

$$Y(j\omega) = \frac{G(j\omega)H(j\omega)N(j\omega) - G_1(j\omega)H(j\omega)S(j\omega) + G_1(j\omega)R(j\omega)}{1 + G(j\omega)H(j\omega)} \quad (4)$$

Assume, for the moment, that the last two terms in the numerator of (4) are negligible. We will justify this assumption below. Then, defining  $T(j\omega)$  as:

$$T(j\omega) = \frac{Y(j\omega)}{N(j\omega)} = \frac{G(j\omega)H(j\omega)}{1 + G(j\omega)H(j\omega)} \quad (5)$$

and:

$$G(j\omega)H(j\omega) = \frac{T(j\omega)}{1 - T(j\omega)} \quad (6)$$

If our assumption can be shown to be valid and we can measure  $T(j\omega)$ , then we can obtain the open-loop gain  $G(j\omega)H(j\omega)$  analytically! Examination of Equation (5) tells us that over the range where  $G(j\omega)H(j\omega)$  is large,  $T(j\omega)$  is nearly unity and we have relaxed the dynamic range required of the test equipment and simplified the achievement of a high signal-to-noise ratio for the measurement.

If we analyze the output of the added summing node,  $Z(j\omega)$ , we find:

$$Z(j\omega) = Y(j\omega) - N(j\omega) = \frac{-N(j\omega)}{1 + G(j\omega)H(j\omega)} + \frac{G_1(j\omega)R(j\omega) - G_1(j\omega)H(j\omega)S(j\omega)}{1 + G(j\omega)H(j\omega)} \quad (7)$$

Since the normal situation within the band of interest is that  $G(j\omega)H(j\omega) \gg 1$  Equation (7) implies that the test signal  $N(j\omega)$  will have negligible affect on the controlled variable  $C(j\omega)$ . This is particularly true if the summing node is placed such that  $G_2(j\omega)$  is small and the amplitude of  $N(j\omega)$  is selected to be small compared to the nominal operating point. The measurement can be made with the control system on line and operating. Proper conditioning of  $N(j\omega)$  has the additional advantage that the system will usually behave linearly in spite of the presence of non-linearities.

We have now overcome most of the objections listed above, except those associated with using a sinusoidal stimulus. It also remains to justify the assumption made in arriving at Equation (5). Returning to Equation (4) and choosing as the test signal,  $N(j\omega)$ , random noise supplied by the 5420A, we see that our assumption that the last two terms of the numerator are negligible can be justified. This is true because, with sufficient averaging, the 5420A will discriminate against signals which are not phase coherent with the input. While a random test signal is not necessary, it is optimum since it correlates least of all with any other signal.

There are other substantial advantages which accrue from using a random stimulus. Noise, with its broadband spectrum, excites all frequencies of interest simultaneously and, since the 5420A detects all frequencies simultaneously, the effects of long time constants are avoided. Measurement time can be dramatically decreased even if one performs extensive averaging. Distortion products, generated by system non-linearities, will not be coherent with the input and will be discriminated against. The result is an estimate of a good linear approximation to the transfer function of non-linear system.<sup>1</sup> As a final point, the approximately Gaussian amplitude distribution of the 5420A's noise generator provides a good simulation of a system operating in a small range about a nominal operating point.

## The Closed-Loop Function

In addition to the open-loop transfer function  $G(j\omega)H(j\omega)$ , we normally have an interest in the closed-loop function  $C(j\omega)/R(j\omega)$  defined by Equation (1). If  $H(j\omega)$  is a constant or is otherwise known, then the closed-loop function can be obtained analytically from our previous measurement of  $T(j\omega)$ . If  $H(j\omega)$  is not known, it is normally possible to re-define the system output to include it or to measure it using the 5420A. Finally, it is usually possible to measure  $C(j\omega)/R(j\omega)$  directly with the 5420A. In the latter case, assuming one is interested,  $H(j\omega)$  can be derived from the measurements of  $C(j\omega)/R(j\omega)$  and  $T(j\omega)$ .

## A General Illustration

The circuit shown in Figure 3 was built to provide a convenient means of illustrating the application of the 5420A to the study of feedback control systems. It represents a control circuit with three independent poles, unity feedback, and variable open-loop gain. Since the circuit has unity feedback it is a simple matter to study both the open- and closed-loop gain.

An analysis of the circuit yields:

$$G(j\omega)H(j\omega) = \frac{(2.77 \times 10^8)(K)}{(j\omega + 5555)(j\omega + 500)(j\omega + 100)} \quad (8)$$

for the open-loop gain where  $K$  represents the variable gain of the final stage. The closed-loop gain,  $C(j\omega)/R(j\omega)$  is obtained from Equation (1) as:

$$\frac{C(j\omega)}{R(j\omega)} = \frac{2.77 \times 10^8(K)}{(j\omega)^3 + 6155(j\omega)^2 + 3.37 \times 10^6(j\omega) + 2.27 \times 10^8(1+K)} \quad (9)$$

Necessary connections to the 5420A for the measurement of  $T(j\omega)$  are shown in the figure. The design of the summing node circuitry is covered in Appendix A.

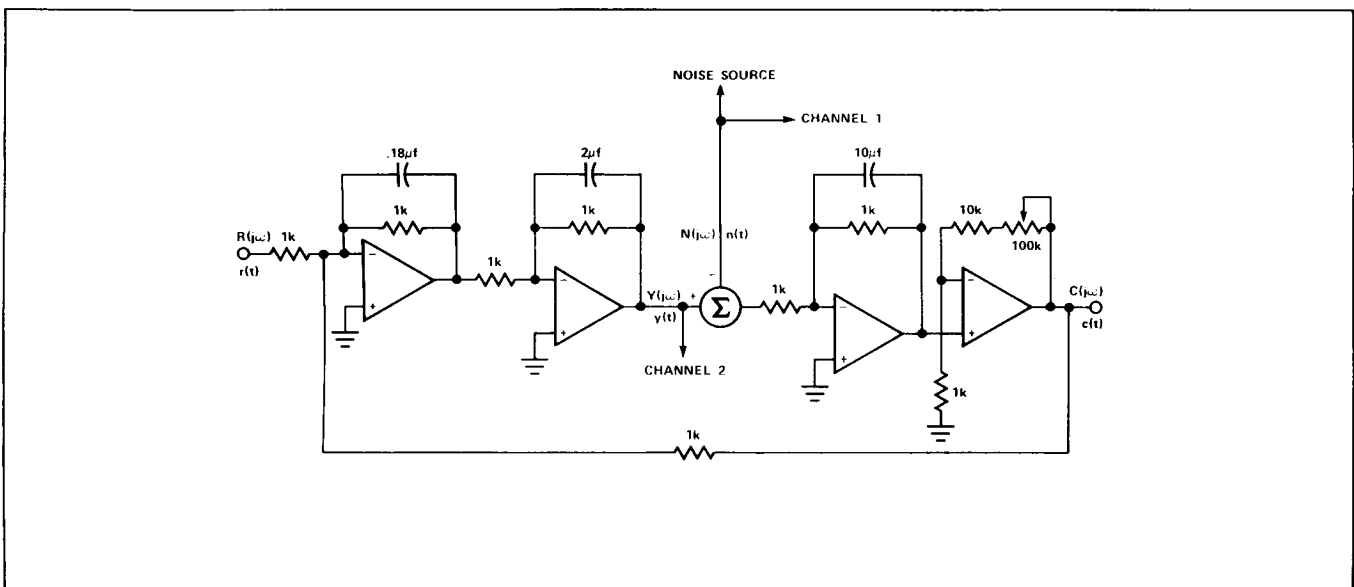


Figure 3

<sup>1</sup>It is important to note, when dealing with non-linearities, that the test signal must be truly random if discrimination against distortion products is to be achieved. Pseudo-random noise is a poor test signal when non-linearity is present and will frequently yield invalid results. The noise supplied by the 5420A is true random noise.

## FREQUENCY DOMAIN MEASUREMENTS

Measurements of  $T(j\omega)$  were made at three different gain settings. Figure 4 illustrates the direct measurement of  $T(j\omega)$  which, in this case, also represents the closed-loop gain.

$$G(j\omega)/[1+G(j\omega)H(j\omega)]$$

The 'waveform calculator' built into the 5420A allows the user to add, subtract, multiply and divide complete functions appearing on the dual-trace display. It also allows the operator to enter real or complex constants for use in his calculations and to multiply or divide by powers of  $j\omega$ . Measured or calculated functions may be stored on the internal digital cartridge and automatically recalled for use in computation. It is a simple task, requiring only a few keystrokes, to compute the open-loop gain from the measurement of  $T(j\omega)$  using Equation (6).

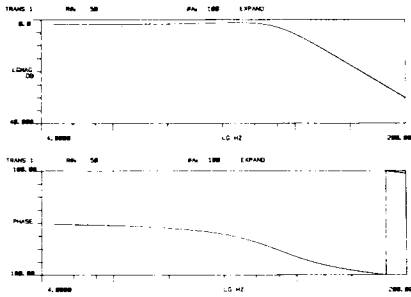


Figure 4a

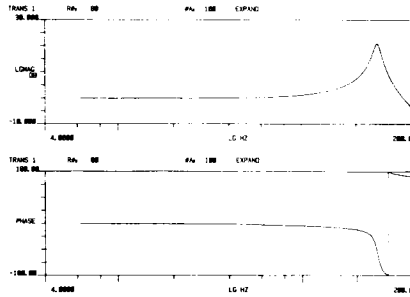


Figure 4b

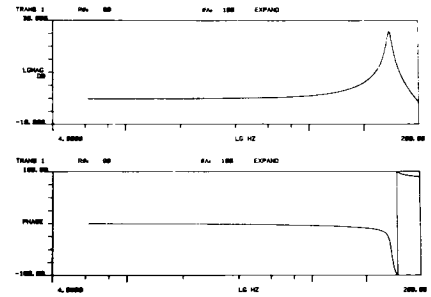


Figure 4c

The results, at three gain settings, are shown in Bode format (log magnitude versus log frequency) in Figure 5. While the shape of the open-loop function does not change significantly with increasing gain, the corresponding closed-loop functions are clearly different.

The open-loop data of Figure 5 is displayed in Nyquist (Imaginary versus Real) format in Figure 6. As we expect, increasing gain drives the system closer to instability until, in Figure 6C, the plot passes through the critical point and the circuit oscillates.

Figure 7 illustrates the open-loop data plotted in Nichols (log magnitude versus phase) coordinates so that the decreasing gain and phase margins can be easily observed. In Figure 7, a cursor has been placed at 180 degrees and the magnitude of the gain margin, together with the frequency at which it occurs, are read from the display.

The 5420A's 'waveform calculator' can be used to synthesize transfer functions of arbitrary complexity. There are several practical applications of this capability when designing control systems. If an analytical expression for the open- or closed-loop gain is available (e.g., Equations (8) and (9)), the actual measured result can be compared to the expected results. The effects of gain and component changes are easily investigated and the results to be expected from compensation networks can be explored prior to building and testing the actual hardware.

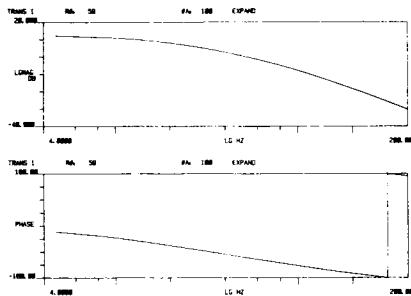


Figure 5a

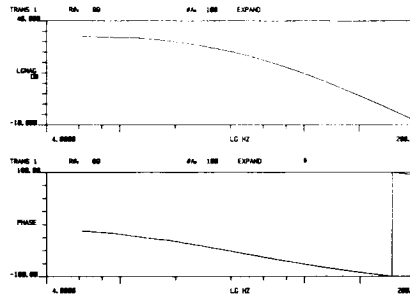


Figure 5b

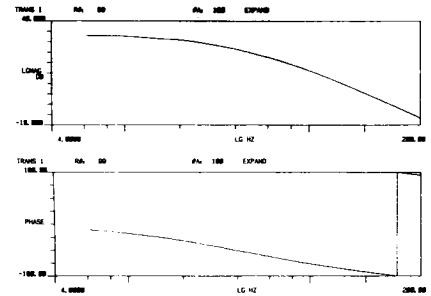


Figure 5c

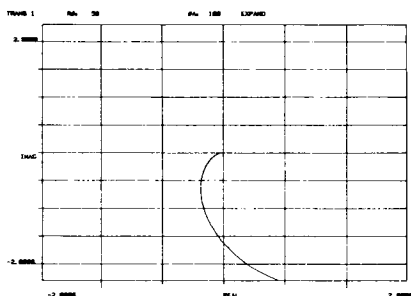


Figure 6a

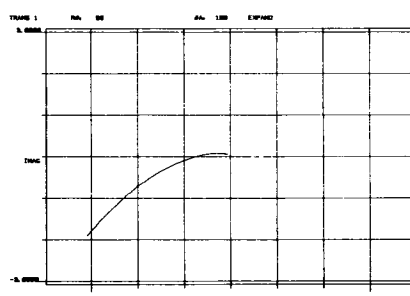


Figure 6b

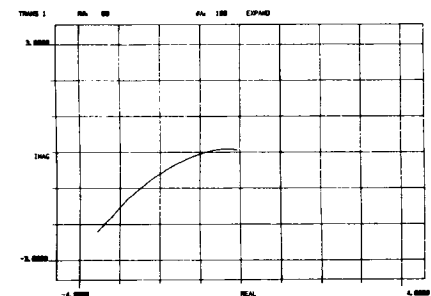


Figure 6c

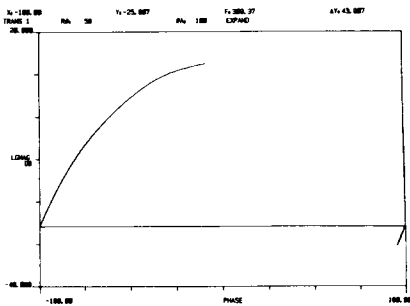


Figure 7a

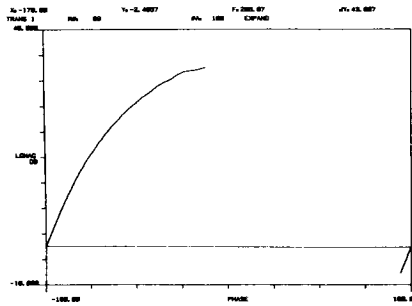


Figure 7b

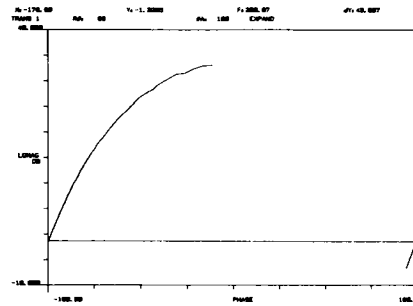


Figure 7c

As a simple example, suppose we desire to determine the result of adding the phase lead network in Figure 8 to our test circuit. We will use the measured data shown in Figures 4B and 5B as the starting point. The phase lead network has a transfer function given by

$$\frac{j\omega(\alpha\tau)+1}{\alpha[j\omega(\tau)+1]} = \frac{j\omega(0.0025)+1}{2[j\omega(0.00125)+1]} \quad (10)$$

where

$$\tau = \frac{R_1 R_2 C}{R_1 + R_2} = 0.00125 \text{ and } \alpha = \frac{R_1 + R_2}{R_2} = 2$$

Equation (10) is easily evaluated using the arithmetic capabilities of the 5420A. The result (magnitude and phase) is shown in Figure 9. The next step is to multiply the synthesized compensation function by the measured open-loop function of Figure 5B. Finally, Equation (1) is used to compute the compensated closed-loop function. The result is shown as the solid trace in Figure 10 with the uncompensated function from Figure 4B overlaid as the dashed trace for comparison.

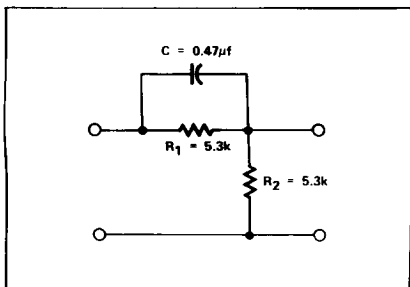


Figure 8

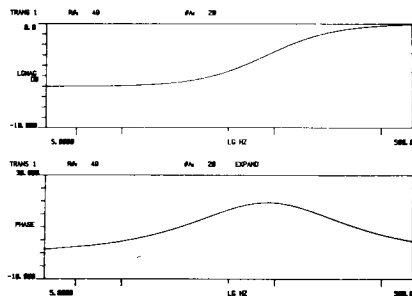


Figure 9

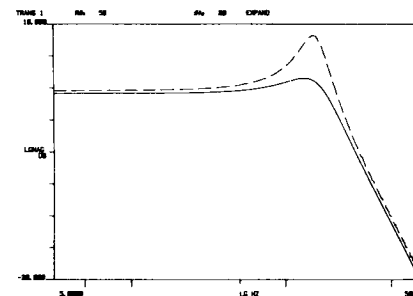


Figure 10

## TIME DOMAIN MEASUREMENTS

The 5420A is also well suited to the examination of the time domain behavior of feedback systems. The closed-loop impulse response of the test circuit at the various gain settings is shown in Figure 11. In Figure 11C, the X and Y axis cursors have been positioned about an area of interest to be expanded. The expanded display is shown in Figure 12 and clearly shows that the circuit is unstable. The 5420A automatically computes impulse response from the measured closed-loop transfer function.

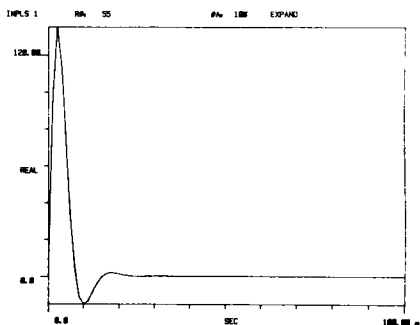


Figure 11a

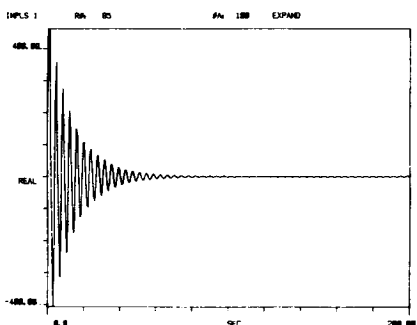


Figure 11b

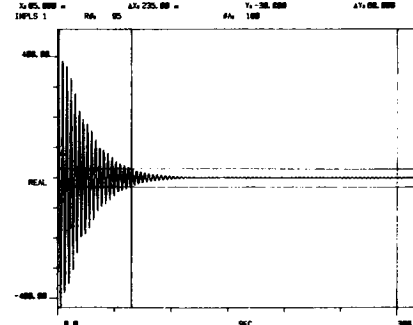


Figure 11c

As a second illustration of time domain studies, the instrument was used to measure the step response of the test circuit. The data was taken with the noise signal  $n(t)$ , set to zero. The input,  $r(t)$ , was driven with a step function and the resulting output,  $c(t)$ , was observed in the time domain. The pre-trigger delay capability of the 5420A was used to insure that the entire transient, including the leading edge, was captured.

The results are shown in Figure 13 for the different gain settings. Note that Figure 13C shows an output which occurred for no input and verifies the frequency domain prediction that the circuit is oscillating.

The time domain parameters of interest are easily determined. For example, Figure 14 shows the step response of Figure 13A with the calibration of the vertical axis converted to percent. This is quickly accomplished by using the Y-axis cursor to read the steady-state level of the response and the 'waveform calculator' to divide the data by this value and to multiply by 100. The Y-axis cursors can then be explicitly set to, say, the 10% and 90% points and the X-axis cursors positioned to read the rise time, as shown in Figure 14. Direct reading of the percent overshoot is illustrated in Figure 15.

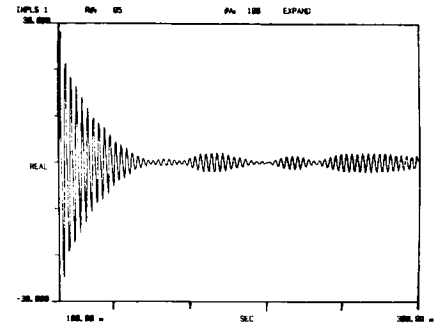


Figure 12

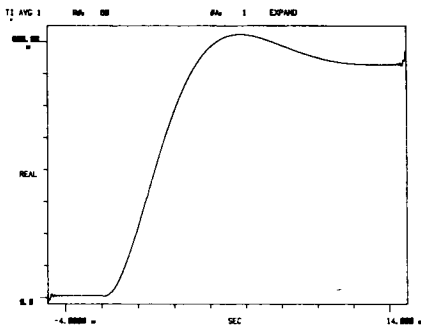


Figure 13a

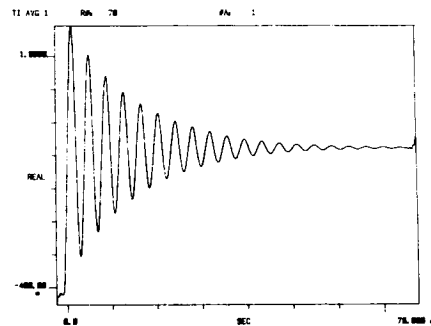


Figure 13b

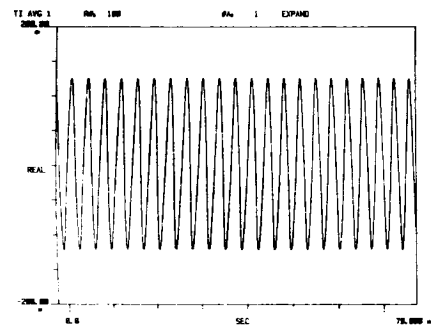


Figure 13c

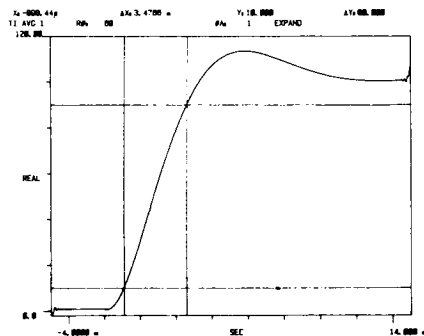


Figure 14

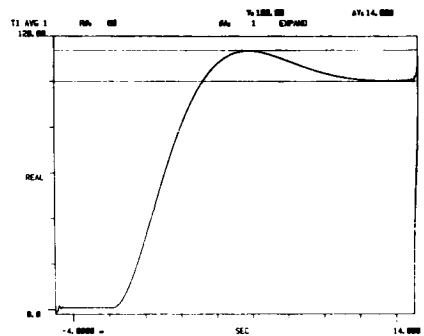


Figure 15

## Tape Speed Control

As a practical example of the characterization of feedback systems, consider the speed control diagrammed in Figure 16. It is used to achieve constant tape speed in the 5420A's cartridge tape drive which is driven by an armature controlled permanent magnet dc motor. An analog feedback signal is obtained by filtering the output of an optical pulse tachometer. The set point input,  $R(j\omega)$ , represents a command for the motor to run at constant speed. System noise, represented by  $S(j\omega)$ , is contributed several elements including unregulated motor voltage, mechanical imbalances, and varying frictional forces.

The measurement of  $T(j\omega)$  is shown in Figure 17. If we consider the tach signal to be the system output, then  $T(j\omega)$  represents the closed-loop gain. The open-loop gain is shown in Figure 18, and we note that the system is stable.



It is frequently of interest to examine the relationship between the controlled variable and system noise  $S(j\omega)$ . It can be shown from Figure 1 that this relationship is given by:

$$F(j\omega) = \frac{C(j\omega)}{S(j\omega)} = \frac{1}{1 + G(j\omega)H(j\omega)} = 1 - T(j\omega)$$

which is, of course, easily evaluated using the 5420A. In our example it represents the attenuation applied by the control loop to the perturbations such as mechanical imbalance, discussed above. The result is shown in Figure 19.

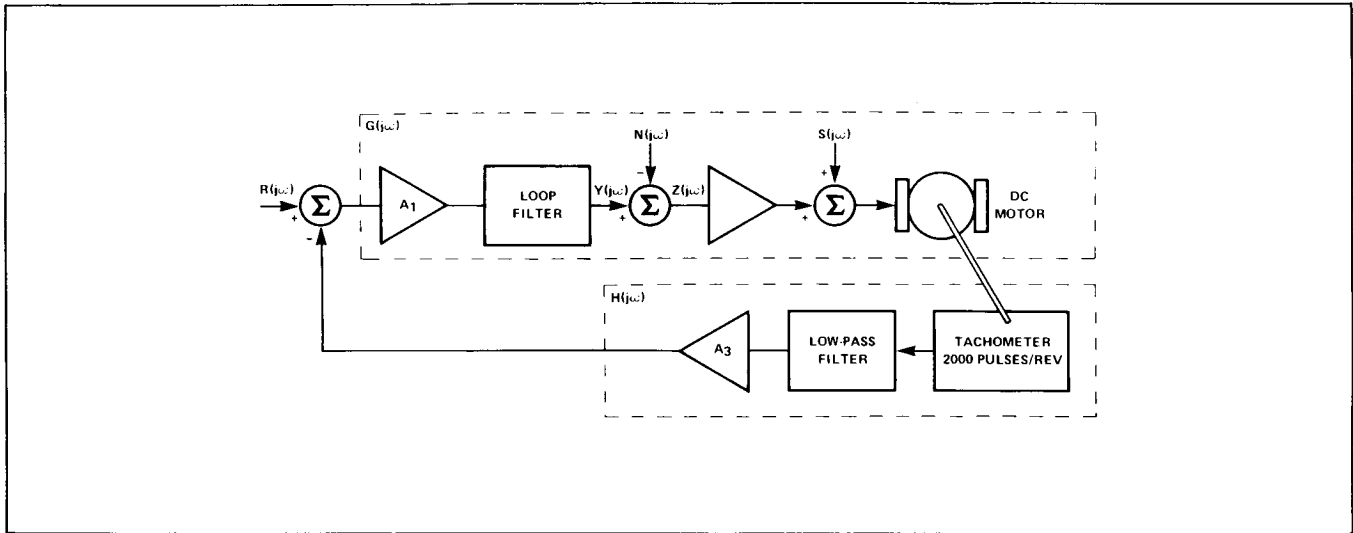


Figure 16

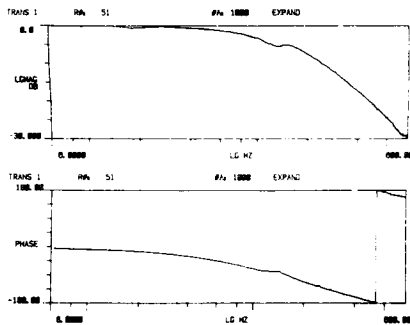


Figure 17

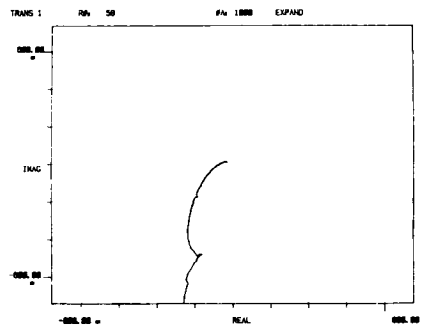


Figure 18

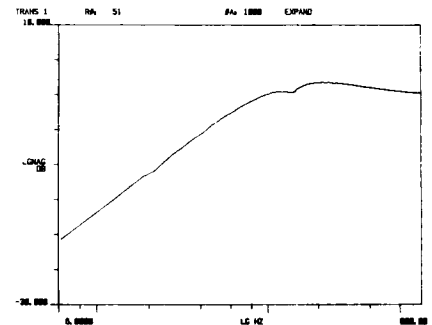


Figure 19

## Head Positioning Servo

As a final example of the usefulness of the closed-loop technique, Figure 20 illustrates a measurement of  $G(j\omega)H(j\omega)$  made on the head positioning servo of the high-performance, 50 M-byte disc drive diagramed in Figure 21. The unit tested was an early prototype in which incompatibility between the recording medium and the head support gimbal caused the track follower servo loop to generate an audio tone.

Examination of each of the peaks shown in Figure 20 revealed that the resonance at about 5 kHz was the cause of the instability (Figure 22). The transfer function of each mechanical component in the positioning loop was measured using appropriate transducers. This data revealed the cause of the problem to be radial motion of the head gimbal. A structural re-design of the gimbal was undertaken to shift the frequency and reduce the amplitude of the resonance.

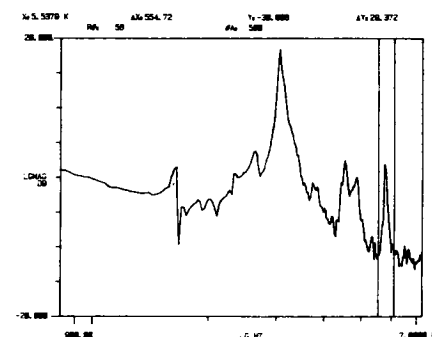


Figure 20

The 5420A is well suited to measuring transfer functions of mechanical components and, therefore, to providing the information needed to solve problems associated with unwanted vibration. The instrument is adaptable to any of the commonly used testing techniques<sup>2</sup> and maintains data calibration even when working with transducers. Its Band Selectable Analysis capability provides the frequency resolution needed to characterize even the sharpest mechanical resonances.

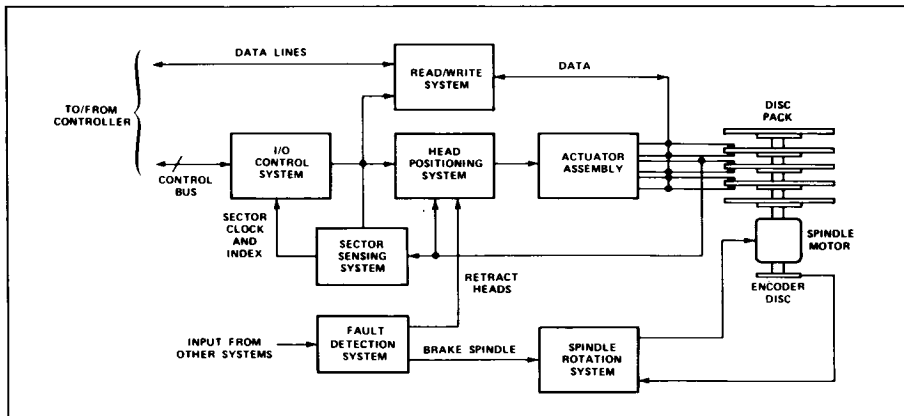


Figure 21

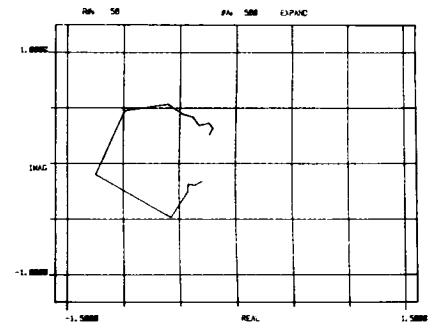


Figure 22

## Conclusions

A modern digital signal analyzer such as the Hewlett-Packard Model 5420A offers a number of substantial benefits which can significantly ease the task of characterizing closed-loop control systems. Among those we have attempted to illustrate are:

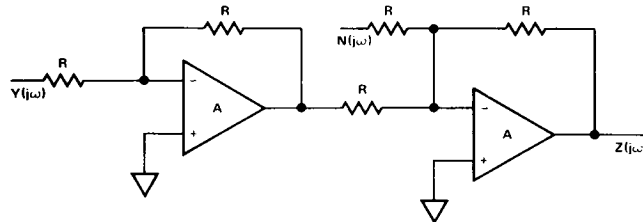
- The ability to make both time and frequency domain measurements with a single instrument, thus ensuring that complete information is available.
- The ability to characterize the system with the loop closed and operating which can simplify the measurement problem and provides for a realistic evaluation under near normal conditions.
- The ability to utilize a complex test signal such as true random noise which can offer a number of advantages including simultaneous measurements at all frequencies of interest. This can reduce test time and also allows the operator to conveniently observe the effect of adjustments made on the system under test.
- The ability to display calibrated results in the most useful format at the push of a key, thus eliminating labourious calculation.
- The ability to compute parameters of interest, such as the disturbance factor  $F(j\omega)$  and the closed-loop impulse response from a single set of measured data. These measurements are frequently difficult or impossible to make directly and, in any event, are time consuming and require changes to the test setup.
- The ability to synthesize transfer functions of arbitrary complexity and to use such functions to compare predicted to actual performance and to explore the suitability of proposed compensation techniques without the requirement that the network actually be built and tested.
- The ability to rapidly characterize mechanical, as well as electronic, components of a control system via transfer function measurements, thus providing a complete design tool.
- The ability to permanently store measured data, in a compact digital form, for later recall and display, further processing, or simply as a permanent record. This capability frequently eliminates the need to repeat time consuming measurements when a need for additional information arises.
- The ability (optional) to obtain fully annotated, four-color graphic and alphanumeric hard copy of either measured or computed functions for use in reports or as a permanent record.
- Finally, while not illustrated in this note, the Hewlett-Packard 5420A when equipped with the 10920A HP-IB Interface, can be remotely controlled by an external calculator or computer. It can also pass data to the controller for additional processing or accept data from the controller for processing, display, or plotting. In this fashion, the already considerable capabilities of the instrument can be greatly extended and the user can easily adapt it to meet particular requirements.

<sup>2</sup>See: Ramsey, K.A., "Effective Measurements for Structural Dynamics Testing Part II," Sound and Vibration Magazine, April 1976, Volume 10, No. 4.

## SUMMING NODE DESIGN AND GENERAL MEASUREMENT CONSIDERATIONS

Many of the measurements illustrated in this note were made using the circuit in Figure A to implement the summing node. The circuit is useful as long as operational amplifiers with adequate voltage range, drive capability and bandwidth can be found. It is important that the summing node not alter the performance of the system in which it is used. Depending on how tightly the system is operating, this may require close attention to good design practice and impedance levels, high-quality amplifiers, and carefully matched components.

As is the case with any measurement technique, the methods outlined cannot be successfully applied without careful consideration and a good understanding of the particular control system to be characterized. Both the design and the placement of the summing node deserve attention. Signal levels should always be optimized using the VIEW INPUT mode of the 5420A. Maintaining adequate signal-to-noise ratio and frequency resolution over the band of interest may require that the Band Selectable Analysis (Zoom) capability of the 5420A be invoked and the measurement made in two or more passes. Band Selectable Analysis can offer several important advantages in particular situations. Among them are adequate resolution to follow rapid gain changes such as may occur in the open-loop gain at low frequency or to identify closely spaced resonances which may occur anywhere in the band of interest. In addition, BSA results in a higher signal-to-noise ratio for the measurement.



02-5952-7098

HEWLETT  PACKARD

Printed in U.S.A.